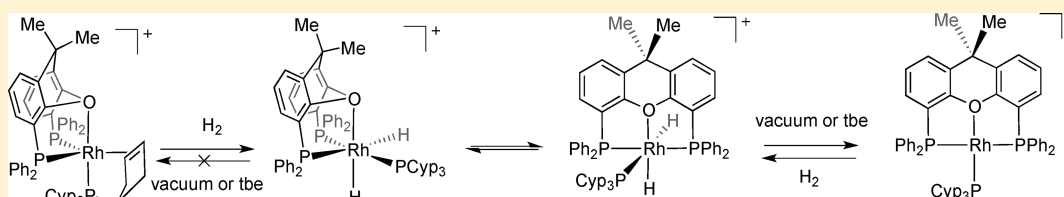


Rhodium Cyclopentyl Phosphine Complexes of Wide-Bite-Angle Ligands DPEphos and Xantphos

Romaeo Dallanegra, Adrian B. Chaplin, and Andrew S. Weller*

Department of Chemistry, Inorganic Chemistry Laboratories, University of Oxford, Oxford, OX1 3QR, U.K.

Supporting Information



ABSTRACT: Rh(I) and Rh(III) complexes of tricyclopentylphosphine (PCyp₃), or its dehydrogenated variant PCyp₂(η^2 -C₅H₇), partnered with wide-bite-angle chelating diphosphine ligands DPEphos and Xantphos have been prepared and characterized in solution and the solid state with the aim of studying their potential for reversible dehydrogenation of the PCyp₃ ligand. The complexes *fac*-[Rh(κ^3 -P,O,P-L){PCyp₂(η^2 -C₅H₇)}][BAR^F₄] (L = DPEphos, Xantphos) show pseudo-trigonal-bipyramidal structures in which the dehydrogenated phosphine alkene ligand acts in a chelating manner. Addition of H₂ to *fac*-[Rh(κ^3 -P,O,P-DPEphos){PCyp₂(η^2 -C₅H₇)}][BAR^F₄] resulted in an equilibrium mixture of hydride and hydride-dihydrogen complexes, *fac*-[Rh(κ^3 -P,O,P-DPEphos)(H)₂(PCyp₃)][BAR^F₄] and [Rh(κ^2 -P,P-DPEphos)(η^2 -H₂)(H)₂(PCyp₃)][BAR^F₄], in which the DPEphos acts as a hemilabile ligand. For the more rigid Xantphos ligand two dihydride isomers, *fac*-[Rh(κ^3 -P,O,P-Xantphos)(H)₂(PCyp₃)][BAR^F₄] and *mer*-[Rh(κ^3 -P,O,P-Xantphos)(H)₂(PCyp₃)][BAR^F₄], are formed, which are also in equilibrium with one another. A van't Hoff analysis of this mixture shows that enthalpically there is very little difference between the two geometries for this system, with the driving force for the preferred *fac*-geometry being entropic. Addition of MeCN to these hydrido complexes results in the central oxygen atom being displaced to form [Rh(κ^2 -P,P-L)(PCyp₃)(H)₂(MeCN)][BAR^F₄], while removal of H₂ from the hydrido complexes (under vacuum or on addition of a hydrogen acceptor) forms the Rh(I) complexes [Rh(κ^3 -P,O,P-L)(PCyp₃)][BAR^F₄], which are characterized as having square-planar geometries with meridional coordination of the respective chelating phosphines. Dehydrogenation of the PCyp₃ ligand in these complexes to re-form the phosphine–alkene ligands does not occur, even under forcing conditions.

INTRODUCTION

We have recently reported on the rhodium-mediated dehydrogenation¹ of cyclopentylphosphine, or cyclopentyl thioether, ligands to form hybrid chelating Lewis-base/alkene ligands (Chart 1a). For example treatment of the complex Rh{Ph₂P(CH₂)₂PPh₂}₂(PCyp₃)Cl with Na[BAR^F₄] results in the rapid, acceptorless, dehydrogenation of one of the cyclopentyl groups to form [Rh{Ph₂P(CH₂)₂PPh₂}₂{PCyp₂(η^2 -C₅H₇)}][BAR^F₄] **A** [Cyp = *cyclo*-C₅H₉; Ar^F = C₆H₃-3,5-(CF₃)₂] (Chart 1b).^{2,3} Analogously, addition of S-CypPh to [Rh{Ph₂P(CH₂)₃PPh₂}₂(η^6 -C₆H₄F₂)][BAR^F₄] forms Rh{Ph₂P(CH₂)₃PPh₂}₂{SPh(η^2 -C₅H₇)}][BAR^F₄] **B**.⁴ These processes can also occur in the solid state,⁵ with different supporting ligand sets other than chelating phosphines,^{3,6,7} or metals other than Rh.^{3,8} Competition experiments indicate that the Cyp unit is particularly well set up for dehydrogenation, compared with cyclohexyl or isopropyl substituents.^{3,7} Others (notably the groups of Sabo-Etienne, e.g., **D**,^{9,10} Grützmacher, e.g., **E**,¹¹ and Bergman, e.g., **F**,¹² Chart 1b) have also reported on related dehydrogenations of cyclic alkyl phosphines, using either PCyp₃ or closely related ligands, with or without the requirement for a sacrificial hydrogen acceptor. We have also reported similar

acceptorless dehydrogenation for acyclic phosphines, **C**,¹³ as have others.^{14,15} In some cases the dehydrogenation is fully reversible, and addition of H₂ re-hydrogenates the double bond to re-form the phosphine with a saturated alkyl group.^{3,5,9,11,13} There is also interest in phosphine–alkene and related, hybrid ligands due to roles that they can play in directing metal-mediated catalytic transformations.^{2,16–20}

As previously we have used simple chelating phosphines, such as Ph₂P(CH₂)_nPPh₂ (*n* = 2 or 3), as supporting ligands on the metal center for these dehydrogenation reactions, we were particularly interested in extending our studies to include chelating phosphine ligands which have a wide bite angle, such as DPEphos and Xantphos (DPEphos, bite angle = 101°; Xantphos, 111°;²¹ Chart 2). These ligands have been shown to promote catalysis through a combination of steric and electronic factors.^{21–23} Moreover we,²⁴ and others,²⁵ have demonstrated the hemilabile role^{26–28} that DPEphos can play in catalytic processes, being able to interconvert between a

Special Issue: F. Gordon A. Stone Commemorative Issue

Received: October 25, 2011

Published: January 6, 2012

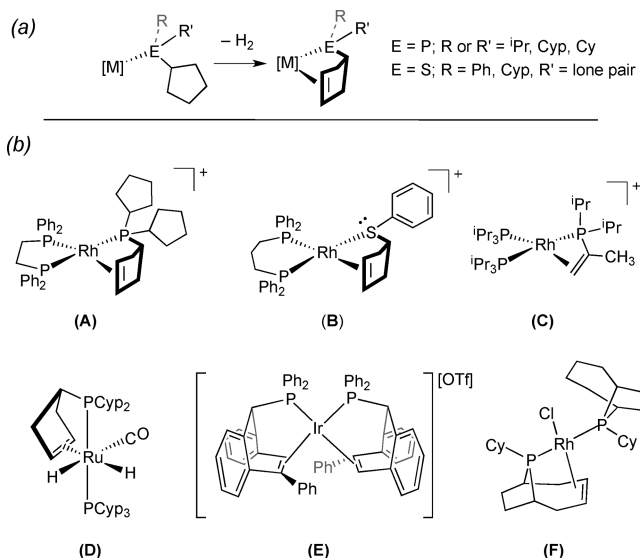
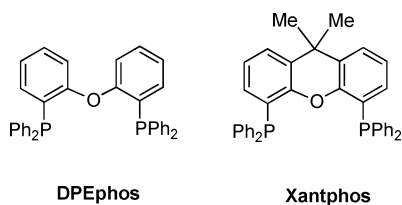
Chart 1^a^a[BAR^F₄] anions not shown.

Chart 2

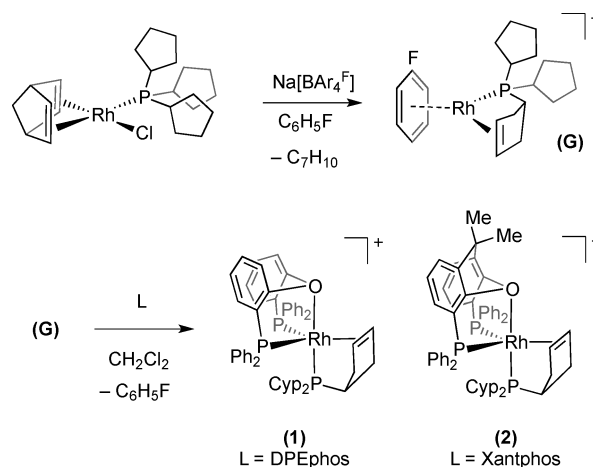


bidentate κ^2 -P,P-coordination mode and a tridentate κ^3 -P,O,P pincer ligand-like coordination geometry (either *fac* or *mer*). In a similar manner, Xantphos can also adopt a number of different coordination modes.²⁹ Such flexible behavior might promote C–H activation and β -hydrogen transfer through the generation of a suitable *cis* vacant site on the metal center, steps both necessary for dehydrogenation of alkyl phosphines. We were interested to see if all these above factors combined to allow access to a catalytic regime for dehydrogenation of the PCyp₃ ligand. To this end, this paper reports on an investigation of the coordination chemistry of PCyp₃, and its dehydrogenated variant PCyp₂(η^2 -C₅H₇), on Rh(I) and Rh(III) centers also bound with Xantphos and DPEphos.

RESULTS AND DISCUSSION

Synthesis of Complexes [Rh(L){PCyp₂(η^2 -C₅H₇)}][BAR^F₄], L = DPEphos, Xantphos. The Rh(I) diphosphine precursor complex Rh(DPEphos)(PCyp₃)Cl was first targeted as a suitable precursor to *fac*-[Rh(DPEphos){PCyp₂(η^2 -C₅H₇)}][BAR^F₄] (**1**), by analogy with Rh{Ph₂P(CH₂)₂PPh₂}(PCyp₃)Cl, which forms [Rh(Ph₂P(CH₂)₂PPh₂){PCyp₂(η^2 -C₅H₇)}][BAR^F₄] (**A**) on halide abstraction and subsequent rapid dehydrogenation.³ Unfortunately, despite repeated attempts we were unable to make the required precursor Rh(DPEphos)(PCyp₃)Cl. Instead the direct synthesis of the coordinated dehydrogenated ligand was achieved, by addition of DPEphos to [Rh(η^6 -C₆H₅F){PCyp₂(η^2 -C₅H₇)}][BAR^F₄] (**G**)³ to form *fac*-[Rh(κ^3 -P,O,P-DPEphos){PCyp₂(η^2 -C₅H₇)}][BAR^F₄] (**1**) in quantitative yield. The equivalent Xantphos

complex, *fac*-[Rh(κ^3 -P,O,P-Xantphos){PCyp₂(η^2 -C₅H₇)}][BAR^F₄] (**2**), was isolated in an analogous manner (Scheme 1).

Scheme 1. Synthesis of **1** and **2**^a^a[BAR^F₄] anions are not shown.

Complexes **1** and **2** were characterized by NMR spectroscopy, ESI-MS, microanalysis, and single-crystal X-ray diffraction (Figure 1). These data show that the PCyp-derived ligand remains coordinated to the metal, which adopts a pseudo-trigonal-bipyramidal geometry with the phosphorus atoms of the diphosphine located in equatorial positions *cis* to each other and opposite the alkene, which itself lies in an equatorial orientation, as expected for a formally d⁸ metal center (i.e., Rh(I)) interacting with a π -acceptor with this geometry.^{30,31} The DPEphos and Xantphos oxygen atoms are located in the axial position *trans* to the phosphorus atom of the tricyclopentylphosphine-derived ligand. The Rh–O bond length for **2** is shorter than that of **1** [2.184(2) Å (**2**) vs 2.250(2) Å (**1**)], presumably a result of the more rigid backbone of the Xantphos ligand, compared to DPEphos, which enforces the oxygen atom in a position closer to the metal. That the Rh–P1 distances are the same within error between the two complexes [2.2256(7) Å (**1**) vs 2.2285(8) Å (**2**)], and in solution the Rh–P1 coupling constants of **1** and **2** are similar [145 Hz (**1**); 152 Hz (**2**)], *vide infra*, suggests a similar interaction of the cyclopentyl phosphine in both cases and, thus, similar Rh–O bond strengths. The C=C bond lengths for the two complexes are also the same within error [1.425(4) Å (**1**) and 1.416(4) Å (**2**)] and are also comparable with complexes **A** and **G** [1.372(3), 1.401(4) Å respectively].³ The P2–Rh1–P3 angle is larger in **2** than in **1** [118.17(3)^o versus 110.83(2)^o, respectively], reflecting the larger bite angle of the Xantphos ligand. Five-coordinate Rh(I) species are known as both cationic^{32,33} and neutral species.^{33–35}

In both complexes the coordinated alkene is confirmed by diagnostic signals in their respective ¹H NMR spectra: δ 3.84 (2H) (**1**); 3.58 (2H) (**2**) (cf. δ 3.89 Å). Complex **2** also shows two inequivalent methyl environments for the Xantphos ligand, δ 1.86 (s, 3H), 1.37 (s, 3H). The ¹³C{¹H} NMR spectra also demonstrate the coordination of an alkene unit [δ 74.9 (br) (**1**); δ 62.2 (dd, *J* = 22, 12 Hz) (**2**)]. These shifts are broadly similar to previously reported phosphine–alkene complexes, e.g., **A** and **G**, δ 96.2 and 65.0, respectively.³ The ³¹P{¹H} NMR spectra show an A₂MX spin system for both **1** and **2**, with two mutually coupled phosphorus environments observed in a 1:2

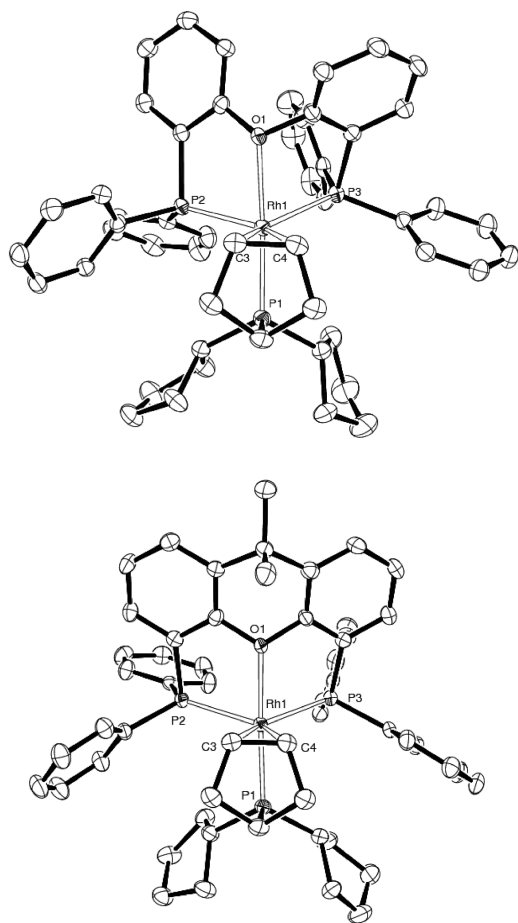


Figure 1. Solid-state structure of the cationic portion of **1** and **2**. Hydrogen atoms are omitted for clarity. Thermal ellipsoids are presented at the 50% probability level. Selected bond lengths [Å] and angles [deg], **1**: Rh1–P1 2.2256(7), Rh1–P2 2.3270(7), Rh1–P3 2.3969(7), Rh1–O1 2.250(2), Rh1–C3 2.128(3), Rh1–C4 2.175(3), C3–C4 1.425(4); P1–Rh1–P2 101.00(2), P1–Rh1–P3 108.95(2), P2–Rh1–P3 110.83(2); **2**: Rh1–P1 2.2285(8), Rh1–P2 2.4007(7), Rh1–P3 2.3529(7), Rh1–O1 2.184(2), Rh1–C3 2.151(3), Rh1–C4 2.165(3), C3–C4 1.416(4); P1–Rh1–P2 105.87(3), P1–Rh1–P3 103.63(3), P2–Rh1–P3 118.17(3).

ratio. Relatively small ^{31}P – ^{31}P coupling constants (42 Hz, **1**; 22 Hz, **2**) show that the phosphorus atoms are located *cis* to each other, similar to other Rh(I)–trisphosphine–alkene complexes.³⁶ These solution data are fully consistent with a *fac* geometry for the phosphine ligands, as observed in the solid state, and that the dehydrogenated PCyp ligand is bound tightly to the metal center.

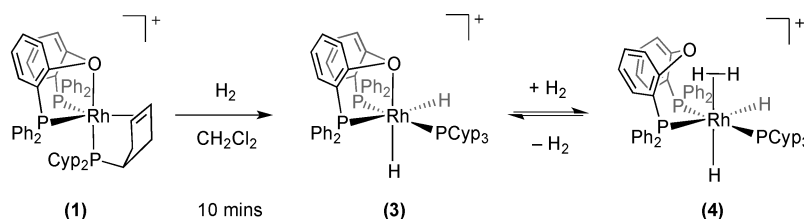
Reactivity of 1 and 2 with H₂. Addition of hydrogen (4 atm, 10 min) to **1** at 298 K in CD₂Cl₂ solution results in the

hydrogenation of the bound alkene, as characterized by the disappearance of the alkene signal in the ^1H NMR spectrum, and the generation of *fac*-[Rh(κ^3 -P,O,P-DPEphos)(H)₂(PCyp₃)] [BAR^F₄] (**3**) (Scheme 2). The ^1H spectrum of complex **3** shows two broad, integral 1H, hydride environments at 298 K, suggesting a slow exchange process at room temperature. On cooling to 223 K, these resolve into complex signals centered at δ –8.66 ppm [apparent doublet of quintets J = 149 Hz, 13 Hz] and –22.95 [apparent triplet, J = 13 Hz], which have not shifted appreciably from those at 298 K. The large ^{31}P – ^1H coupling constant [J = 149 Hz] for the resonance at δ –8.66 ppm shows that this hydride is opposite a phosphorus atom. The $^{31}\text{P}\{^1\text{H}\}$ spectrum at 233 K reveals three environments in a 1:1:1 ratio. Each phosphorus couples to ^{103}Rh as well as two inequivalent phosphorus nuclei, with a pair of phosphorus atoms lying *trans* to each other [$J(\text{PP})$ = 319 Hz] and the remaining phosphorus atom in a mutually *cis* orientation to the others. In addition to these signals, at 223 K under a pressure of H₂ (4 atm) three new broad resonances are observed at δ –1.79 (2H), –10.94 (1H), and –13.18 (1H), which are attributed to the dihydrogen dihydride complex [Rh(κ^2 -P,P-DPEphos)(η^2 -H₂)(H)₂(PCyp₃)] [BAR^F₄] (**4**). The ratio of **3**:**4** is 17:1 at this temperature. Although we have no direct evidence, we assume that, to retain an 18-electron configuration in **4**, the central ether linkage of the DPEphos is not bound and the DPEphos ligand is acting as a hemilabile ligand.^{28–30}

Evidence for a dynamic equilibrium between **3** and **4** was obtained by cooling further to 198 K (500 MHz), whereby the ratio of complexes **3**:**4** changed to 5:1. T_1 relaxation measurements^{37,38} for **4** were also gathered at this temperature. The relative 2 H integral assigned to **4** at δ –1.79 has a measured T_1 of 21 ms (at 500 MHz), consistent with a dihydrogen ligand, while the low-frequency hydride resonances relax at 400 ms, typical of a hydride ligand.^{37,38} These data can be compared with those for the closely related complexes [Rh{Ph₂P(CH₂)₂PPh₂}(η^2 -H₂)(H)₂(PCyp₃)] [BAR^F₄], η^2 -H₂ 19 ms, (H)₂ 215 ms (500 MHz),³ and [Ru(κ^3 -P,O,P-DPEphos)(η^2 -H₂)(H)(PPh₃)] [BAR^F₄], η^2 -H₂ 9.6 ms (400 MHz), (H)₂ 324 ms (400 MHz).³⁹

The solid-state structure of **3**, using crystals obtained by recrystallization under H₂ (*vide infra*), is consistent with the NMR spectroscopic data for this complex and shows a distorted six-coordinate octahedral geometry. Both hydride ligands were located in the final difference map (Figure 2). The tricyclopentylphosphine ligand is located *trans* to one phosphorus atom of the DPEphos ligand (which itself adopts a *fac* geometry at the metal center), and one of the hydride ligands lies *trans* to the other phosphorus atom of the diphosphine. The Rh–O distance [2.308(2) Å] is longer than in **1**, consistent with the high *trans* influence of the hydride,

Scheme 2^a



^a[BAR^F₄] anions not shown.

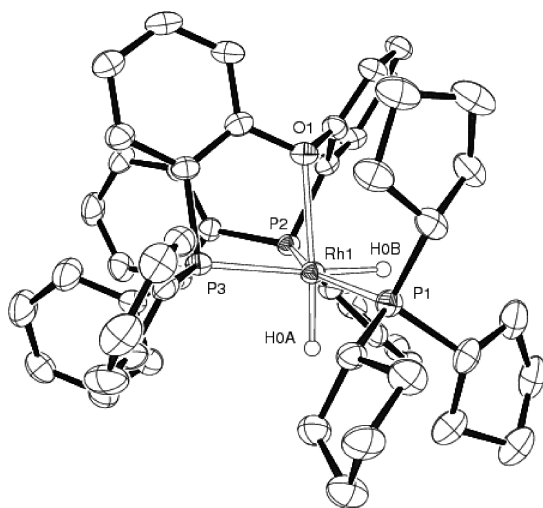


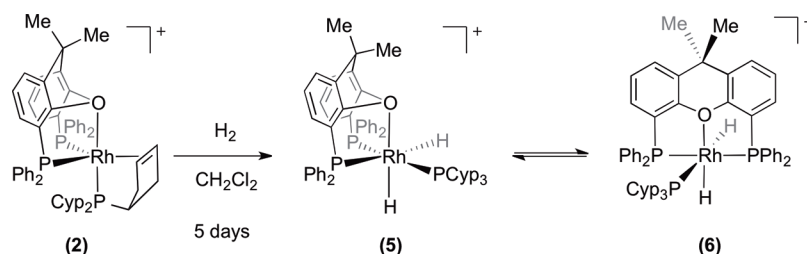
Figure 2. Solid-state structure of the cationic portion of **3**. Hydrogen atoms (except hydride ligands) are omitted for clarity. Thermal ellipsoids are presented at the 50% probability level. Selected bond lengths [Å] and angles [deg]: Rh1–P1 2.3135(10), Rh1–P2 2.3349(10), Rh1–P3 2.3514(10), Rh1–O1 2.308(2), Rh1–H0A 1.49(4), Rh1–H0B 1.54(3); P1–Rh1–P2 153.78(4), P1–Rh1–P3 106.99(4), P2–Rh1–P3 99.20(3), O1–Rh1–P1 104.07(7), O1–Rh1–P2 78.42(7), O1–Rh1–P3 81.12(6).

especially given the move from Rh(I) to smaller Rh(III) in **3**. By contrast Rh–P3 is not significantly longer than Rh–P2 [2.3514(10) versus 2.3349(10) Å] even though P3 is also *trans* to a hydride. These similar bond lengths are reflected in similar ^{103}Rh – ^{31}P coupling constants for the phosphines (104–114 Hz) in solution. This suggests that the bound oxygen ligand is more susceptible to *trans* ligand influence than the phosphine, which is consistent with the fact that it can be displaced by H_2 .

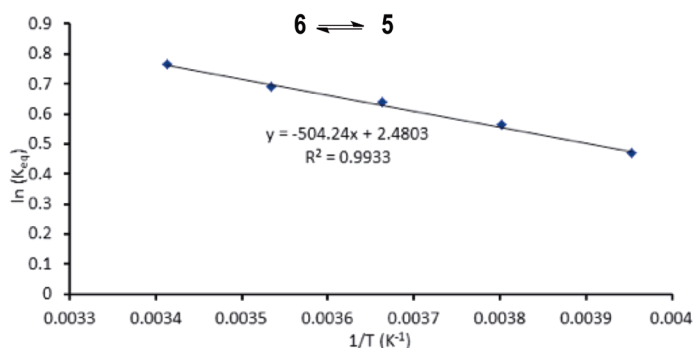
At 298 K complex **2** undergoes hydrogenation considerably slower than **1** (5 days compared with 10 min). Two dihydride isomers, *fac*-[Rh(κ^3 -P,O,P-Xantphos)(H) $_2$ (PCyp $_3$)] [BAr F_4] (**5**) and *mer*-[Rh(κ^3 -P,O,P-Xantphos)(H) $_2$ (PCyp $_3$)] [BAr F_4] (**6**), are formed (Scheme 3), unlike DPEphos, which gives rise to only the *fac*-isomer. As breaking the Rh–O bond and coordination of H_2 in **1** and **2** is presumably the first step in these reactions, prior to oxidative cleavage of H_2 , this difference in reaction time supports a stronger or, at the very least, less flexible nature of the Rh–O bond in **2** compared to **1**. No dihydrogen complex was observed for Xantphos.

The ^1H NMR spectra of **5** and **6** at room temperature are characterized by pairs of complex multiplet hydride environments at room temperature in a 2.2:1 ratio of **5**:**6**, reflecting the formation of two isomers: δ –9.33, –22.19 (**5**) and δ –7.93, –20.49 (**6**). The signals at δ –9.33 (**5**) and –7.93 (**6**) show distinctive *trans* coupling to ^{31}P , $J(\text{PH}) = 143$ and 135 Hz, respectively, as confirmed by $^1\text{H}\{^{31}\text{P}\}$ experiments. The signals due to **5** were broadened slightly, compared to **6**, which are sharp at 298 K. The wide difference in chemical shifts between the two hydride environments of each complex reflects the nature of the substituent located *trans* to the hydride: phosphorus or less strongly bound oxygen.⁴⁰ The room-temperature $^{31}\text{P}\{^1\text{H}\}$ spectrum exhibits three broadened phosphorus environments for **5** (1:1:1 ratio), two of which display both *cis* and *trans* ^{31}P – ^{31}P coupling, while only two sharp signals (2:1 ratio) are observed for **6**, which show only *cis* coupling. Upon cooling a solution containing a mixture of **5** and **6** from 293 to 253 K, the relative integrals of the hydride resonances changed slightly from 1:2.2 **6**:**5** to 1:1.7 **6**:**5**. This suggests the presence of an equilibrium between the two species. Moreover at low temperature, NMR signals due to **5** sharpen considerably. There is no significant change in chemical shifts on cooling. The hydride resonances were successfully simulated using gNMR⁴¹ as an ABMXYZ system in

Scheme 3^a



$$\Delta G(298) = -1.9 \pm 0.4 \text{ kJmol}^{-1}; \Delta H = +4.4 \pm 0.2 \text{ kJmol}^{-1}; \Delta S = +21.3 \pm 0.6 \text{ J K}^{-1}\text{mol}^{-1}$$



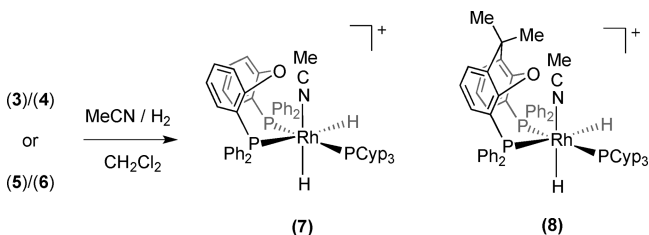
^a[BAr F_4] anions not shown.

5 and an ABMX₂Y system in 6. Overall, these data support the assigned κ^3 -*fac* and κ^3 -*mer* coordination geometries for 5 and 6, respectively, with the κ^3 -*mer* isomer preferred marginally over the κ^3 -*fac*. We suggest that the isomerization may occur via decoordination of the central oxygen atom to reveal a five-coordinate intermediate.

A van't Hoff plot (Scheme 3) for the equilibrium between 6 and 5 yields a straight line, from which the enthalpy of $+4.4 \pm 0.2$ kJ mol⁻¹ and entropy, $+21.3 \pm 0.6$ J K⁻¹ mol⁻¹, associated with this equilibrium were determined, giving an overall $\Delta G(298\text{ K}) = -1.9 \pm 0.4$ kJ mol⁻¹ for 6 to 5. These data show that enthalpically there is very little difference between the κ^3 -*fac* and κ^3 -*mer* geometries in this system, and the driving force for the preferred *fac* geometry in this particular case is entropic. Although Xantphos can be considered to be a κ^3 -meridional-coordinating ligand,^{29,39,42–47} examples of κ^3 -*fac* coordination are also known.^{29,42} Neither are that common, however, compared to the κ^2 -P,P coordination mode.⁴⁸ The broadening of the NMR signals of 5 at room temperature might suggest the ability to access greater conformational freedom compared to 6, consistent with an increase in entropy. As the relative order of these thermodynamic parameters for this *fac* over *mer* preference are likely to be rather system-specific, we are reluctant to generalize this result to other Xantphos complexes.

The results so far reported suggest that 16-electron, low-coordinate, intermediates are accessible, probably via O-decoordination in the DPEphos and Xantphos compounds. To explicitly probe this, an excess of MeCN (10 equivalents) was added to CH₂Cl₂ solutions of mixtures of complexes 3/4 and 5/6 under an atmosphere of H₂, to avoid loss of H₂ from the metal center (*vide infra*). This afforded *mer*-[Rh(κ^2 -P,P-DPEphos)(PCyp₃)(H)₂(MeCN)][BAR^F₄] (7) and *mer*-[Rh(κ^2 -P,P-Xantphos)(PCyp₃)(H)₂(MeCN)][BAR^F₄] (8), respectively, in quantitative yield by NMR spectroscopy (Scheme 4). The

Scheme 4^a



^a[BAR^F₄] anions not shown.

formation of 7 and 8 was demonstrated by the observation of three separate environments in their respective ³¹P{¹H} NMR spectra, for which a pair of resonances in each show *trans* ³¹P–³¹P coupling. In the ¹H NMR spectra of 7 and 8, two sharp hydride multiplets were observed for each complex. Selective ¹H{³¹P} NMR spectroscopy experiments removed several orders of fine structure in these resonances to reveal the H–H and Rh–H coupling constants for these signals. Large P–H coupling constants, $J(\text{PH}_{\text{trans}}) = 149$ and 149 Hz respectively for 7 and 8, locate one hydride *trans* to a phosphine. Replacement of the ether-oxygen (e.g., 3/4) with a more strongly bound NCMe ligand (e.g., 7) results in a downfield shift of 3–5 ppm for the *trans* hydride, as expected.⁴⁰ These signals were successfully modeled using gNMR (Figure 3). Related κ^3 -P,O,P to κ^2 -P,P geometry changes have been noted

before in DPEphos and Xantphos complexes on reaction with MeCN.^{24,42}

Complexes 3/4 and 5/6 lose H₂ readily. When placed under vacuum or upon addition of the (tbe = tertbutylethene), they form the Rh(I) complexes [Rh(κ^3 -P,O,P-DPEphos)(PCyp₃)]-[BAR^F₄] (9) and [Rh(κ^3 -P,O,P-Xantphos)(PCyp₃)]-[BAR^F₄] (10), respectively, in quantitative yield by NMR spectroscopy (Scheme 5). Complexes 5/6 lose H₂ rapidly (one freeze–thaw–degas cycle), while H₂ loss is much slower for 3/4 (5 cycles). The rapid loss of H₂ for 5/6 meant that the relative rates of disappearance of the *fac* and *mer* isomers could not be measured. It is interesting to note that the Xantphos ligand promotes this reductive elimination faster than DPEphos, although we cannot definitively say whether this is a steric or electronic effect.^{21,23,49}

The ³¹P{¹H} NMR spectra for both 9 and 10 reveal two mutually *cis* phosphorus environments in a 2:1 ratio, which show coupling to a Rh(I) center. The ¹H NMR spectra show no evidence for hydrides, and for 10 a single, 6H, methyl environment is observed for the Xantphos ligand. The solid-state structures of 9 and 10 demonstrate square-planar geometries (sum of the angles around the Rh center = 359.99° and 361.15°, respectively) (Figure 4). The chelating phosphorus atoms approach a *trans* configuration [$156.61(5)^\circ$ (9); $158.409(7)^\circ$ (10)]. The Rh–O bond distance in 9 is significantly shorter than in 1 [$2.189(3)$ Å vs $2.2503(17)$ Å (1)] on moving to this Rh(I) square-planar geometry, while that for 10 lengthens compared to 2 [$2.222(5)$ Å (10) vs $2.1837(19)$ Å (2)]. The structural metrics of 9 and 10 compare favorably with other Rh(I) complexes containing κ^3 -P,O,P-*trans* spanning Xantphos-type ligands.^{44,47} Complexes 9 and 10 do not react further with respect to the bound PCyp₃ ligand, and no dehydrogenation (via C–H activation/ β -hydrogen transfer) is observed even under forcing conditions in the presence of a hydrogen acceptor (tbe, 313 K). By contrast complexes 9 and 10 react with H₂ (4 atm) to re-form mixtures of 3/4 and 5/6, respectively, as monitored by NMR spectroscopy.

CONCLUSIONS

We have studied a number of rhodium complexes of the tricyclopentylphosphine ligand partnered with wide-bite-angle chelating diphosphine ligands DPEphos and Xantphos. Our initial hopes that these ligands would support dehydrogenation of the PCyp₃ ligand were not realized due to the relatively strong κ^3 -P,O,P binding of the chelate diphosphine ligand, at least compared to a weak C–H agostic bond that would precede the desired C–H activation. Instead we have shown that the Xantphos ligand is actually rather flexible, for example, with *fac*- κ^3 -P,O,P and *mer*- κ^3 -P,O,P geometries closely matched in terms of enthalpy, with entropy playing an unexpected role in determining the overall position of equilibrium between the two. As each conformation has a different ligand bite angle associated with the metal center (i.e., *fac*- κ^3 -P,O,P 107° in 3, *mer*- κ^3 -P,O,P 156° in 10), it is tempting to suggest that the ability for the ligand to adopt both coordination geometries (and be in equilibrium between them) might have a significant bearing on other metal-centered processes that are intimately linked to the relative demands of the phosphines, such as the relative rates of hydride insertion into an alkene or reductive elimination.²³

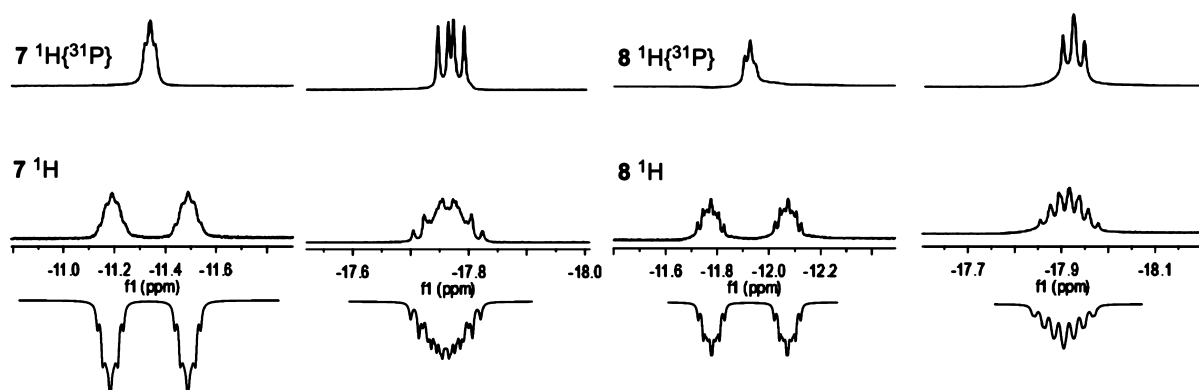
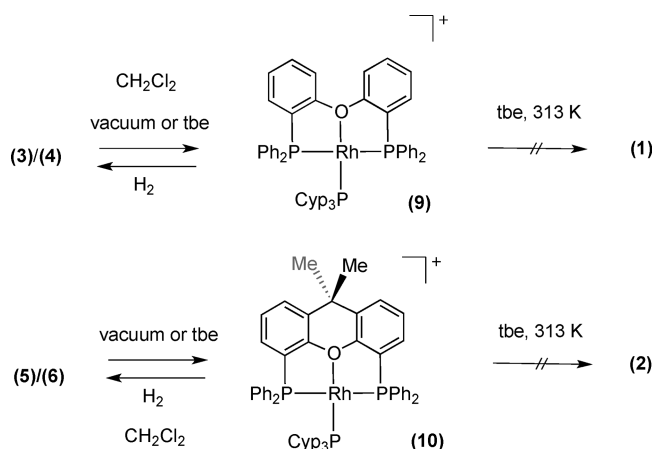


Figure 3. Experimental and simulated ^1H and $^1\text{H}\{^{31}\text{P}\}$ NMR spectra for 7 and 8.

Scheme 5^a



^a[BAR^{F}_4] anions not shown.

EXPERIMENTAL SECTION

All manipulations, unless otherwise stated, were performed under an atmosphere of argon, using standard Schlenk and glovebox techniques. Glassware was oven-dried at 130 °C overnight and flamed under vacuum prior to use. CH_2Cl_2 , MeCN, hexane, and pentane were dried using a Grubbs-type solvent purification system (MBraun SPS-800) and degassed by successive freeze–pump–thaw cycles.⁵⁰ CD_2Cl_2 , $\text{C}_6\text{H}_5\text{CF}_3$, and $\text{C}_6\text{H}_5\text{F}$ were distilled under vacuum from CaH_2 and stored over 3 Å molecular sieves. *tert*-Butylethylene was dried over sodium, vacuum distilled, and stored over 3 Å molecular sieves. Microanalyses were performed by Elemental Microanalysis Ltd. NMR spectra were recorded on Varian Unity⁺ 500 MHz or Bruker AVII 500 MHz spectrometers at room temperature unless otherwise stated. Residual protio solvent was used as reference for ^1H and ^{13}C NMR spectra in deuterated solvent samples. ^{31}P NMR spectra were referenced against 85% H_3PO_4 (external). Chemical shifts are quoted in ppm and coupling constants in Hz. Electrospray Ionization mass spectrometry (ESI-MS) was recorded using a Bruker MicrOTOF instrument directly connected to a modified Innovative Technology glovebox.⁵¹ Typical acquisition parameters were as follows: sample flow rate (4 $\mu\text{L}/\text{min}$), nebulizer gas pressure (0.4 bar), drying gas (argon at 60 °C, flowing at 4 L/min), capillary voltage (4.5 kV), funnel voltage (200 V). MS samples were diluted to a concentration of 1×10^{-6} M before running. $[\text{Rh}(\eta^6\text{-C}_6\text{H}_5\text{F})\{\text{PCyp}_2(\eta^2\text{-C}_5\text{H}_7)\}][\text{BAR}^{\text{F}}_4]$, **G**, was prepared by the literature procedure.³ All other chemicals were used as received from Sigma-Aldrich, Acros, Fisher, Fluka, Fluorochem, and Strem Chemicals.

Crystallography. Data were collected on an Enraf Nonius Kappa CCD diffractometer using graphite-monochromated Mo $K\alpha$ radiation ($\lambda = 0.71073$ Å) and a low-temperature device [150(2) K];⁵² data were collected using COLLECT, reduction and cell refinement were

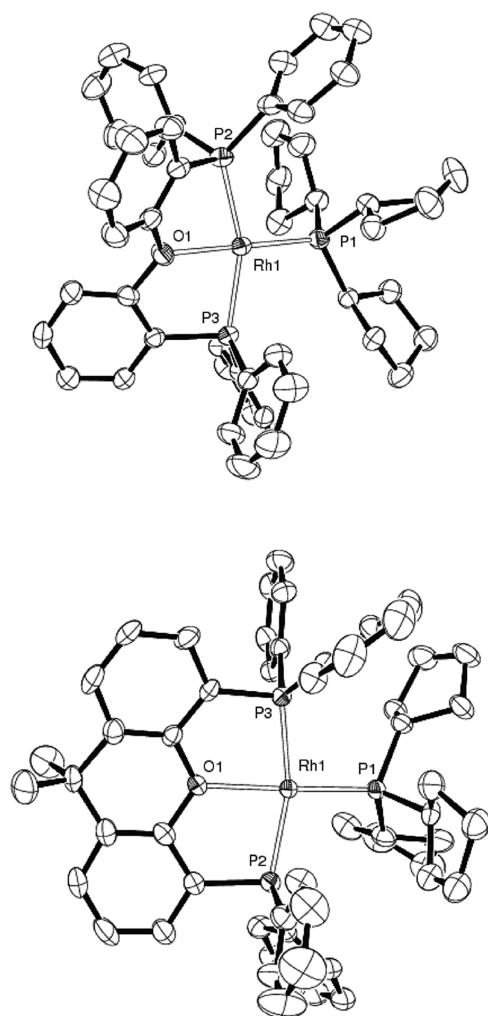


Figure 4. Solid-state structure of the cationic portion of 9 and 10. Hydrogen atoms are omitted for clarity. Thermal ellipsoids are presented at the 50% probability level. Selected bond lengths [Å] and angles [deg], 9: Rh1–P1 2.2375(13), Rh1–P2 2.3247(12), Rh1–P3 2.2678(12), Rh1–O1 2.189(3); P1–Rh1–P2 102.71(5), P1–Rh1–P3 100.67(4), P2–Rh1–P3 156.61(5), O1–Rh1–P1 178.89(10), O1–Rh1–P2 77.27(9), O1–Rh1–P3 79.34(9); 10: Rh1–P1 2.2458(19), Rh1–P2 2.2985(19), Rh1–P3 2.2659(19), Rh1–O1 2.222(5); P1–Rh1–P2 101.07(7), P1–Rh1–P3 97.83(7), P2–Rh1–P3 158.40(7), O1–Rh1–P1 174.08(15), O1–Rh1–P2 80.80(14), O1–Rh1–P3 81.45(14).

Table 1. Crystallographic Data for 1, 2, 3, 9, and 10

	1	2	3	9	10
CCDC	849263	849264	849265	849266	849267
formula	C ₈₃ H ₆₅ BF ₂₄ OP ₃ Rh	C ₈₆ H ₆₉ BF ₂₄ OP ₃ Rh	C ₈₃ H ₆₉ BF ₂₄ OP ₃ Rh.C ₆ H ₅ F	C ₈₃ H ₆₇ BF ₂₄ OP ₃ Rh	C ₈₆ H ₇₁ BF ₂₄ OP ₃ Rh
<i>M</i>	1740.98	1781.04	1841.11	1743.00	1783.06
cryst syst	triclinic	triclinic	triclinic	monoclinic	triclinic
space group	$P\bar{1}$	$P\bar{1}$	$P\bar{1}$	$P2_1/c$	$P\bar{1}$
<i>a</i> [Å]	13.4238(1)	12.8119(1)	13.3042(3)	13.9956(1)	12.8590(1)
<i>b</i> [Å]	14.2954(1)	16.2707(2)	17.7665(3)	33.5274(3)	17.1395(1)
<i>c</i> [Å]	20.7081(2)	20.9044(2)	20.6626(5)	17.8616(2)	21.8146(2)
α [deg]	73.4829(4)	84.2396(4)	111.7567(9)	90	99.1448(4)
β [deg]	84.0057(4)	72.9026(4)	97.3499(8)	108.1544(4)	106.8047(4)
γ [deg]	83.9868(4)	85.5884(4)	94.865(1)	90	100.7042(4)
<i>V</i> [Å ³]	3777.28(5)	4138.93(7)	4452.2(2)	7964.1(1)	4405.40(6)
<i>Z</i>	2	2	2	4	2
density [g cm ⁻³]	1.531	1.429	1.373	1.454	1.344
μ [mm ⁻¹]	0.397	0.364	0.342	0.376	0.342
θ range [deg]	5.09 < θ < 25.03	5.09 < θ < 25.03	3.35 < θ < 25.03	5.10 < θ < 25.03	5.12 < θ < 25.03
reflins collected	24 027	25 833	23 438	25 718	27 541
<i>R</i> _{int}	0.0219	0.0243	0.0337	0.0419	0.0217
completeness	99.0%	98.9%	94.9%	98.8%	98.9%
no. of data/restr/params	13 197/507/1136	14 469/382/1089	14 947/764/1161	13 918/1081/1129	15 395/3812/1365
<i>R</i> ₁ [<i>I</i> > 2 σ (<i>I</i>)]	0.0329	0.0420	0.0510	0.0572	0.0991
<i>wR</i> ₂ [all data]	0.0794	0.1190	0.1435	0.1396	0.2549
GoF	1.030	1.073	1.055	1.042	1.115
largest diff pk and hole [e Å ⁻³]	0.611, -0.473	0.706, -0.399	0.685, -0.646	0.730, -0.688	1.466, -1.161

performed using DENZO/SCALEPACK.⁵³ The structures were solved by direct methods using SIR2004⁵⁴ and refined with full-matrix least-squares on *F*² using SHELXL-97.⁵⁵ All non-hydrogen atoms were refined anisotropically. Hydride and alkene hydrogen atoms were located on the Fourier difference map; restraints were applied to their 1,2 and 1,3 bond distances, and their isotropic displacement parameters were fixed to ride on the parent atoms. Other hydrogen atoms were placed in calculated positions using the riding model. Problematic solvent disorder in 2, 3, and 10 was treated using the SQUEEZE algorithm.⁵⁶ Details of other disorder modeling are documented in the crystallographic information files under the heading *_refine_special_details*. Minor disorder components are omitted from the figures for clarity. Restraints to thermal parameters were applied and were necessary in order to maintain sensible values. Graphical representations of the structures were made using ORTEP3.⁵⁷ Crystallographic data are detailed in Table 1.

fac-[Rh(κ^3 -P,O,P-DPEphos)(P(Cyp)₂(η^2 -C₅H₇))][BARF₄] (1). DPEphos (16.5 mg, 0.031 mmol) was added to a solution of [Rh(η^6 -C₆H₅F){PCyp₂(η^2 -C₅H₇)}][BARF₄] (G) (40 mg, 0.031 mmol) in CH₂Cl₂ (5 mL) and stirred for 2 h. The solvent was removed *in vacuo*, and the residue was washed with pentane (2 × 3 mL) and dried under reduced pressure. Diffusion of pentane into a solution of the residue in C₆H₅F gave 1 as red crystals. (43 mg, 80%).

¹H NMR (500 MHz, CD₂Cl₂): δ 7.73 (m, 8H, BARF₄), 7.56 (br, 4H, BARF₄), 7.50–7.25 (m, 22H, ArH), 7.18 [dd, *J*(PH) 8.5, *J*(HH) 4.4, 2H, POP bridging ArH], 7.06 (m, 4H, POP bridging ArH), 3.84 (s, 2H, HC=CH), 2.04 (br s, 1H, PC₅H₇), 1.84 [apparent t, *J*(PH) 13, 2H, PCyp CH], 1.65–1.30 (m, 16H, PCyp), 1.25–1.00 (m, 4H, PCyp). ³¹P{¹H} NMR (202 MHz, CD₂Cl₂): δ 84.14 [dt, *J*(RhP) 145, *J*(PP_{cis}) 42], 18.99 [dd, *J*(RhP) 134, *J*(PP_{cis}) 42]. ¹³C{¹H} NMR (126 MHz, CD₂Cl₂): δ 162.17 [q, *J*(BC) 51, BARF₄], 160.05 (d, *J* = 12, C₆H₄OP), 135.35 (s, C₆H₄OP), 135.20 (s, BARF₄), 133.59 (d, *J* = 12, C₆H₅), 133.19 (d, *J* = 34, C₆H₅), 132.11 (s, C₆H₄OP), 130.79 (s, C₆H₅), 129.07 [qq, *J*(FC) 32, *J*(BC) 2.9, BARF₄], 129.00 (d, *J* = 9.5, C₆H₅), 126.74 (d, *J* = 32, C₆H₄OP), 126.36 (d, *J* = 4.8, C₆H₄OP), 125.00 [q, *J*(FC) 273, BARF₄], 120.03 (d, *J* = 4.8, C₆H₄OP), 117.87 [sept, *J*(FC) 3.8, BARF₄], 74.90 (br s, C=C), 36.95 [dt, *J*(PC) 23, *J*(PC) 2.9, CH], 36.40 [d, *J*(PC) 2.9, CH₂], 32.31 [d, *J*(PC) 28, CH], 31.56 (s, CH₂), 29.15 (s, CH₂), 25.92 [d, *J*(PC) 8.6, CH₂], 25.49 [d,

J(PC) 9.5, CH₂]. ESI-MS (C₆H₅F, 373 K, 4.5 kV): positive ion *m/z* 877.2298 [M]⁺ (100% calc 877.2359). Anal. Calcd for C₈₃H₆₅B₁F₂₄O₁P₃Rh₁ (1741.003 g mol⁻¹): C, 57.26; H, 3.74. Found: C, 57.56; H, 3.16.

fac-[Rh(κ^3 -P,O,P-Xantphos)(P(Cyp)₂(η^2 -C₅H₇))][BARF₄] (2). Xantphos (22 mg, 0.038 mmol) was added to a solution of [Rh(η^6 -C₆H₅F){PCyp₂(η^2 -C₅H₇)}][BARF₄] (G) (49.5 mg, 0.038 mmol) in CH₂Cl₂ (5 mL) and stirred for 2 h. The solvent was removed *in vacuo*, and the residue was washed with pentane (2 × 3 mL) and dried under reduced pressure. Diffusion of pentane into a solution of the residue in CH₂Cl₂ gave 2 as orange crystals (50 mg, 74%).

¹H NMR (500 MHz, CD₂Cl₂): δ 7.75 (m, 8H, BARF₄), 7.57 (br, 4H, BARF₄), 7.67–7.52 (m, 6H, ArH), 7.51–7.41 (m, 6H, ArH), 7.36–7.19 (m, 8H, ArH), 7.18–7.03 (m, 6H, ArH), 3.58 (s, 2H, HC=CH), 1.86 (s, 3H, CH₃), 1.85–1.17 (m, 21H, PCyp), 1.37 (s, 3H, CH₃), 1.11–0.89 (m, 4H, PCyp). ³¹P{¹H} NMR (202 MHz, CD₂Cl₂): δ 90.66 [dt, *J*(RhP) 152, *J*(PP_{cis}) 22], 26.56 [dd, *J*(RhP) 131, *J*(PP_{cis}) 22]. ¹³C{¹H} NMR (126 MHz, CD₂Cl₂): δ 162.10 [q, *J*(BC) 50, BARF₄], 156.65 (t, *J* = 8.8, C₆H₃OP), 136.36 (t, *J* = 18, C₆H₅), 135.30 (t, *J* = 2.3, C₆H₃OP), 135.14 (s, BARF₄), 133.89 (s, C₆H₃OP), 133.67 (t, *J* = 11, C₆H₅), 133.03 (t, *J* = 7.3, C₆H₅), 132.45 (t, *J* = 6.1, C₆H₅), 130.48 (s, C₆H₅), 130.38 (s, C₆H₅), 129.31 (t, *J* = 4.6, C₆H₅), 129.21 [qq, *J*(FC) 31, *J*(BC) 3.1, BARF₄], 129.10 (t, *J* = 4.2, C₆H₅), 127.88 (s, C₆H₃OP), 127.27 (s, C₆H₃OP), 126.09 (dd, *J* = 17, *J* = 14, C₆H₃OP), 124.93 [q, *J*(FC) 272, BARF₄], 117.81 [sept, *J*(FC) 3.8, BARF₄], 62.22 (dd, *J* = 22, *J* = 12, C=C), 36.79 (s), 36.51 [br dt, *J*(PC) 25, *J*(PC) 4.6, CH], 35.24 [d, *J*(PC) 31, CH], 35.18 (s, CH₂), 33.03 (s, CH₃), 30.63 [d, *J*(PC) 5.3], 28.55 (s, CH₂), 25.61 [d, *J*(PC) 9.9, CH₂], 25.10 [d, *J*(PC) 11, CH₂], 22.85 (s, CH₃). ESI-MS (C₆H₅F, 373 K, 4.5 kV): positive ion *m/z* 917.2665 [M]⁺ (100% calc 917.2672). Anal. Calcd for C₈₆H₆₉B₁O₁F₂₄P₃Rh₁ (1781.067 g mol⁻¹): C, 57.99; H, 3.90. Found: C, 58.16; H, 3.72.

fac-[Rh(κ^3 -P,O,P-DPEphos)(H)₂(PCyp₃)](BARF₄) (3) and [Rh(κ^2 -P,P-DPEphos)(H)₂(η^2 -H₂)(PCyp₃)](BARF₄) (4). (3) A solution of 1 (25 mg, 0.0144 mmol) in C₆H₅F (2 mL) was frozen in liquid nitrogen, placed under vacuum and backfilled with H₂, and shaken for 10 min. 4 was observed upon cooling this solution to 198 K at a ratio of 1:5 (3:4) and was characterized by ¹H NMR spectroscopy. Diffusion of hydrogen-saturated pentane into the resulting solution and shaking,

after cooling to 253 K, gave **3** as colorless crystals. Complex **3** loses H₂ when removed from a H₂ atmosphere, and thus microanalytical data were not obtained.

3. ¹H NMR (500 MHz, CD₂Cl₂, 223 K): δ 7.80–7.16 (m, 21H, ArH), 7.75 (m, 8H, BAr^F₄), 7.56 (br, 4H, BAr^F₄), 7.10 (apparent triplet, *J* = 7.7, 1H, ArH), 7.00–6.84 (m, 3H ArH), 6.44 (apparent td, *J* = 8.2, 1.6, 2H, ArH) 5.97 (m, 2H, ArH), 1.80–1.20 (m, 27H, PCyp₃), –8.66 [apparent doublet of quintets *J*(PH_{trans}) 149, *J* = 13, 1H, *T*₁ = 0.52 s, RhH], –22.95 (apparent broad triplet, *J* = 13, 1H, *T*₁ = 0.54 s, RhH). ³¹P{¹H} NMR (202 MHz, CD₂Cl₂, 223 K) δ 62.31 [ddd, *J*(PP_{trans}) 319, *J*(RhP) 114, *J*(PP_{cis}) 18], 34.00 [ddd, *J*(PP) 319, *J*(RhP) 106, *J*(PP_{cis}) 22], 27.71 [apparent dt, *J*(RhP) 104, *J*(PP_{cis}) 20]. ESI-MS (C₆H₅F, 373 K, 4.5 kV): positive ion *m/z*, 879.2352 [M – H₂]⁺ (100%, calcd 879.2515), 881.2477 [M]⁺ (65%, calcd 881.2672).

4. ¹H NMR (500 MHz, CD₂Cl₂, 198 K): δ –1.79 (br s, 2H, *T*₁ = 21 ms), –11.06 [br d, *J*(PH_{trans}) 149, 1H], –13.33 (br, 1H). *T*₁ values for the two hydride resonances are approximately 400 ms at this temperature. Although we did not determine *T*₁ min. values, their relative magnitudes allow for a clear discrimination between hydride and dihydrogen ligands.

[Rh(κ³-P,O,P-DPEphos)(H)₂(PCyp₃)](BAr^F₄) isomers (fac-5/mer-6). A solution of **2** (8 mg, 0.0045 mmol) in CD₂Cl₂ (500 μL) was frozen in liquid nitrogen, placed under vacuum and backfilled with H₂, shaken, and left to stand for 5 days. **5/6** were then characterized by ¹H and ³¹P{¹H} NMR spectroscopy.

5. Selected ¹H NMR (500 MHz, CD₂Cl₂): δ –9.33 [br d, *J*(PH_{trans}) 143, 1H, *T*₁ = 0.25 s, RhH], –22.19 (br, 1H, *T*₁ = 0.22 s, RhH). ³¹P{¹H} NMR (202 MHz, CD₂Cl₂): δ 50.85 [br dd, *J*(PP_{trans}) 319, *J*(RhP) 117], 35.36 [br d, *J*(RhP) 91], 27.34 [br d, *J*(RhP) 95]. ESI-MS (C₆H₅F, 373 K, 4.5 kV): positive ion *m/z*, 919.2696 [M – H₂]⁺ (100%, calcd 919.2828).

6. Selected ¹H NMR (500 MHz, CD₂Cl₂): δ –7.93 [apparent dq, *J*(PH_{trans}) 135, *J*(P_{cis}H) 13, *J*(RhH) 13, *J*(HH) 5.8, 1H, *T*₁ = 0.55 s, RhH], δ –20.49 [apparent multiplet, *J*(P_{cis}H) 28.4, *J*(P_{cis}H) 12.3, *J*(RhH) 19.2, *J*(HH) 5.8, 1H, *T*₁ = 0.43 s, RhH]. *These complex signals were simulated using gNMR to extract the corresponding spectral parameters. ³¹P{¹H} NMR (202 MHz, CD₂Cl₂): δ 36.89 [dd, *J*(RhP) 114, *J*(PP_{cis}) 20], 20.71 [dt, *J*(RhP) 97, *J*(PP_{cis}) 20].

[Rh(κ²-P,P-DPEphos)(PCyp₃)(H)₂(MeCN)](BAr^F₄) (7**).** A solution of **1** (8 mg, 0.0046 mmol) in C₆H₅F (500 μL) was frozen in liquid nitrogen, placed under vacuum and backfilled with H₂, and shaken for 10 min to give **3**. MeCN (2 μL) was added, and the product was immediately characterized *in situ* by ¹H and ³¹P{¹H} NMR spectroscopy at 298 K.

¹H NMR (500 MHz, CD₂Cl₂): δ 7.74 (m, 8H, BAr^F₄), 7.57 (br, 4H BAr^F₄), 7.56–7.37 (m, 12H, ArH), 7.34 (br t, 3H, ArH), 7.28–6.96 (m, 9H, ArH), 6.91 (br t, *J* = 7.3, 1H, ArH), 6.63 (br t, *J* = 7.1, 1H, ArH), 6.45–6.27 (m, 2H, ArH), 1.75–1.16 (m, 30H, PCyp₃ and coordinated MeCN), –11.34 [apparent doublet of quintets, *J*(PH_{trans}) 149, *J*(P_{cis}H) 16.7, *J*(P_{cis}H) 11.7, *J*(RhH) 14.4, *J*(HH) 8.5, 1H, RhH], –17.76 [apparent multiplet, *J*(P_{cis}H) 17.2, *J*(P_{cis}H) 14.6, *J*(P_{cis}H) 12.0, *J*(RhH) 10.4, *J*(HH) 8.5, 1H, RhH]. *These complex signals were simulated using gNMR to extract the corresponding spectral parameters. ³¹P{¹H} NMR (202 MHz, CD₂Cl₂): δ 50.85 [dd, *J*(PP_{trans}) 357, *J*(RhP) 110], 32.08 [dd, *J*(PP_{trans}) 358, *J*(RhP) 112], 22.88 [d, *J*(RhP) 99]. ESI-MS (C₆H₅F, 373 K, 4.5 kV): positive ion *m/z*, 879.2380 [M – MeCN – H₂]⁺ (100% calcd 879.2515), 922.2783 [M]⁺ (10% calcd 922.2937). ESI-MSMS of peak 922.2783 *m/z* (C₆H₅F): 881.2528 [M – MeCN]⁺ (calcd 881.2672), 879.2338 [M – MeCN – H₂]⁺ (calcd 879.2515).

[Rh(κ²-P,P-Xantphos)(PCyp₃)(H)₂(MeCN)](BAr^F₄) (8**).** A solution of **2** (8 mg, 0.0045 mmol) in CD₂Cl₂ (500 μL) was frozen in liquid nitrogen, placed under vacuum and backfilled with H₂, shaken, and left for 5 days to yield **5/6**. MeCN (2 μL) was added, and the product was immediately characterized *in situ* by ¹H and ³¹P{¹H} NMR spectroscopy at 298 K.

¹H NMR (500 MHz, CD₂Cl₂): δ 7.72 (m, 8H, BAr^F₄), 7.63 (ddd, *J* = 10.7, 7.7, 1.2, 2H, ArH), 7.56 (m, 4H, BAr^F₄), 7.47–7.36 (m, 6H, ArH), 7.33 (m, 2H, ArH), 7.28–6.99 (m, 14H, ArH), 6.74 (m, 1H, C₆H₃OP), 6.30 (m, 1H, C₆H₃OP), 1.92 (s, 3H, CH₃), 1.85–1.19 (m,

27H, PCyp₃), 1.38 (s, 3H, CH₃), –11.92 [apparent multiplet, *J*(P_{trans}H) 149, *J*(P_{cis}H) 17.3, *J*(P_{cis}H) 14.3, *J*(RhH) 10.8, *J*(HH) 9.2, 1H, RhH], –17.92 [apparent septet, *J*(P_{cis}H) 21.1, *J*(P_{cis}H) 12.5, *J*(RhH) 10.6, *J*(P_{cis}H), *J*(RhH) 9.2, *J*(HH) 7.3, 1H, RhH]. *These complex signals were simulated using gNMR to extract the corresponding spectral parameters.

³¹P{¹H} NMR (202 MHz, CD₂Cl₂): δ 56.59 [ddd, *J*(PP_{trans}) 365, *J*(RhP) 115, *J*(PP_{cis}) 15], 20.03 [ddd, *J*(PP_{trans}) 365, *J*(RhP) 110, *J*(PP_{cis}) 20], 15.27 [ddd, *J*(RhP) 92, *J*(PP_{cis}) 20, *J*(PP_{cis}) 15]. ESI-MS (1,2-C₆H₄F₂, 333 K, 4.5 kV): positive ion *m/z*, 919.2881 [M – MeCN – H₂]⁺ (100% calcd 919.2828).

[Rh(κ³-P,O,P-DPEphos)(PCyp₃)](BAr^F₄) (9**).** A solution of **1** (25 mg, 0.0144 mmol) in C₆H₅F (2 mL) was frozen in liquid nitrogen, placed under vacuum and backfilled with H₂, and shaken for 10 min to give **3**. The H₂ atmosphere was removed under vacuum by freeze/pump/thaw of the solution three times followed by addition of 5 μL of 3,3-dimethylbut-1-ene. The solvent was then removed under reduced pressure, and the resulting residue was washed with pentane (2 × 3 mL) and dried *in vacuo*. An orange crystal suitable for X-ray diffraction was obtained by diffusion of pentane into a solution of **9** in C₆H₅CF₃. Despite repeated attempts, isolation of significant solid material proved unsuccessful as the complex (although pure by NMR spectroscopy) remained an oil.

¹H NMR (500 MHz, CD₂Cl₂): δ 8.28 (br, 2H, ArH), 7.96–7.43 (m, 20H, ArH), 7.75 (m, 8H, BAr^F₄), 7.58 (br, 4H BAr^F₄), 7.29 (apparent td, *J* = 7.3, 1.6, 2H, ArH), 7.16 (t, *J* = 7.6, 2H, ArH), 6.91 (br dt, *J* = 8.4, 2.0, 2H, ArH) 1.90–0.88 (m, 27H, PCyp₃). ³¹P{¹H} NMR (202 MHz, CD₂Cl₂): δ 48.84 [dt, *J*(RhP) 190, *J*(PP_{cis}) 35], 33.42 [dd, *J*(RhP) 156, *J*(PP_{cis}) 35]. ¹³C{¹H} NMR (126 MHz, CD₂Cl₂): δ 162.31 [q, *J*(BC) 50, BAr^F₄], 158.38 (t, *J* = 6.9, C₆H₄OP), 135.93 (br m, C₆H₅), 135.35 (s, BAr^F₄), 133.64 (br m, C₆H₅), 133.39 (s, C₆H₄OP), 132.43 (s, C₆H₄OP), 132.01 (br m, C₆H₅), 129.62 (t, *J* = 5.0, C₆H₅), 129.41 [qq, *J*(FC) 31, *J*(BC) 3, BAr^F₄], 126.62 (t, *J* = 3.1, C₆H₄OP), 125.14 [q, *J*(FC) 272, BAr^F₄], 118.02 [sept, *J*(FC) 3.8, BAr^F₄], 115.57 (t, *J* = 2.3, C₆H₄OP), 40.97 [d, *J*(PC) 29, CH], 30.39 (br m, CH₂), 24.84 (br m, CH₂). ESI-MS (C₆H₅F, 373 K, 4.5 kV): positive ion *m/z*, 879.2429 [M]⁺ (100%, calcd 879.2515).

[Rh(κ³-P,O,P-Xantphos)(PCyp₃)](BAr^F₄) (10**).** A solution of **2** (25 mg, 0.0144 mmol) in C₆H₅F (2 mL) was placed under 4 atm of H₂, shaken, and left for 5 days to yield **5/6**. The H₂ was removed under vacuum by freeze/pump/thaw of the solution. The solvent was then removed under reduced pressure, and the resulting residue was washed with pentane (2 × 3 mL) and dried *in vacuo*. A crystal of **10** suitable for X-ray diffraction was obtained by diffusion of pentane into a solution of the residue in C₆H₅F. Despite repeated attempts, isolation of significant solid material proved unsuccessful, as the complex (although pure by NMR spectroscopy) remained an oil.

¹H NMR (500 MHz, CD₂Cl₂): δ 7.98 (m, 8H, ArH), 7.74 (br, 8H, BAr^F₄), 7.58 (m, 10H, BAr^F₄ and ArH), 7.51 (m, 8H, ArH), 7.29 (m, 2H, C₆H₃OP), 7.21 (t, 2H, *J* = 7.7, C₆H₃OP), 1.63 (s, 6H, CH₃), 1.61 (br m, 3H, PCyp₃), 1.48 (br m, 6H, PCyp₃), 1.31 (br m, 12H, PCyp₃), 0.99 (br m, 6H, PCyp₃). ³¹P{¹H} NMR (202 MHz, CD₂Cl₂): δ 44.33 [dt, *J*(RhP) 193, *J*(PP_{cis}) 35], 33.08 [dd, *J*(RhP) 156, *J*(PP_{cis}) 35]. ¹³C{¹H} NMR (126 MHz, CD₂Cl₂): δ 162.10 [q, *J*(BC) 50, BAr^F₄], 153.05 (t, *J* = 8.1, C₆H₃OP), 135.13 (s, BAr^F₄), 134.13 (t, *J* = 6.9, C₆H₅), 133.44 (s, C₆H₃OP), 132.44 (t, *J* = 22, C₆H₅), 131.56 (s, C₆H₅), 131.40 (t, *J* = 3.1, C₆H₃OP), 130.96 (s, C₆H₃OP), 129.32 (t, *J* = 5.0, C₆H₅), 129.20 [qq, *J*(FC) 31, *J*(BC) 2.7, BAr^F₄], 126.79 (t, *J* = 2.7, C₆H₃OP), 126.46 (t, *J* = 16, C₆H₃OP), 124.93 [q, *J*(FC) 272, BAr^F₄], 117.80 [sept, *J*(FC) 3.8, BAr^F₄], 42.22 [br d, *J*(PC) 29, CH], 34.26 (s, q), 33.55 (s, CH₃), 30.60 (s, CH₂), 25.00 [d, *J*(PC) 11, CH₂]. ESI-MS (C₆H₅F, 373 K, 4.5 kV): positive ion *m/z*, 919.2708 [M]⁺ (100% calcd 919.2828).

■ ASSOCIATED CONTENT

Supporting Information

This material is available free of charge via the Internet at <http://pubs.acs.org>.

■ AUTHOR INFORMATION

Corresponding Author

*E-mail: andrew.weller@chem.ox.ac.uk.

■ ACKNOWLEDGMENTS

We thank the EPSRC and the University of Oxford for support

■ DEDICATION

Dedicated to the memory of Prof. F. Gordon A. Stone.

■ REFERENCES

- (1) Grellier, M.; Sabo-Etienne, S. *Chem. Commun.* **2011**, 48, 34.
- (2) Douglas, T. M.; Notre, J. L.; Brayshaw, S. K.; Frost, C. G.; Weller, A. S. *Chem. Commun.* **2006**, 3408.
- (3) Douglas, T. M.; Brayshaw, S. K.; Dallanegra, R.; Kociok-Kohn, G.; Macgregor, S. A.; Moxham, G. L.; Weller, A. S.; Wondimagegn, T.; Vadivelu, P. *Chem.—Eur. J.* **2008**, 14, 1004.
- (4) Dallanegra, R.; Pilgrim, B. S.; Chaplin, A. B.; Donohoe, T. J.; Weller, A. S. *Dalton Trans.* **2011**, 40, 6626.
- (5) Douglas, T. M.; Weller, A. S. *New J. Chem.* **2008**, 32, 966.
- (6) Molinos, E.; Brayshaw, S. K.; Kociok-Kohn, G.; Weller, A. S. *Dalton Trans.* **2007**, 4829.
- (7) Dallanegra, R.; Chaplin, A. B.; Tsim, J.; Weller, A. S. *Chem. Commun.* **2010**, 46, 3092.
- (8) Moret, S. v.; Dallanegra, R.; Chaplin, A. B.; Douglas, T. M.; Hiney, R. M.; Weller, A. S. *Inorg. Chim. Acta* **2010**, 363, 574.
- (9) Bolton, P. D.; Grellier, M.; Vautravers, N.; Vendier, L.; Sabo-Etienne, S. *Organometallics* **2008**, 27, 5088.
- (10) Grellier, M.; Vendier, L.; Sabo-Etienne, S. *Angew. Chem., Int. Ed.* **2007**, 46, 2613.
- (11) Piras, E.; Läng, F.; Rügger, H.; Stein, D.; Wörle, M.; Grützmacher, H. *Chem.—Eur. J.* **2006**, 12, 5849.
- (12) Lewis, J. C.; Berman, A. M.; Bergman, R. G.; Ellman, J. A. *J. Am. Chem. Soc.* **2008**, 130, 2493.
- (13) Chaplin, A. B.; Poblador-Bahamonde, A. I.; Sparkes, H. A.; Howard, J. A. K.; Macgregor, S. A.; Weller, A. S. *Chem. Commun.* **2009**, 244.
- (14) Glaser, P. B.; Tilley, T. D. *Organometallics* **2004**, 23, 5799.
- (15) Esteruelas, M. A.; López, A. M. *Organometallics* **2005**, 24, 3584.
- (16) Defieber, C.; Grützmacher, H.; Carreira, E. M. *Angew. Chem., Int. Ed.* **2008**, 47, 4482.
- (17) Puschmann, F. F.; Grützmacher, H.; Bruin, B. d. *J. Am. Chem. Soc.* **2010**, 132, 73.
- (18) Shintani, R.; Duan, W.-L.; Nagano, T.; Okada, A.; Hayashi, T. *Angew. Chem., Int. Ed.* **2005**, 44, 4611.
- (19) Lewis, J. C.; Bergman, R. G.; Ellman, J. A. *Acc. Chem. Res.* **2008**, 41, 1013.
- (20) Thaler, T.; Guo, L.-N.; Steib, A. K.; Raducan, M.; Karaghiosoff, K.; Mayer, P.; Knochel, P. *Org. Lett.* **2011**, 13, 3182.
- (21) Freixa, Z.; van Leeuwen, P. W. N. M. *Dalton Trans.* **2003**, 1890.
- (22) van Leeuwen, P. W. N. M.; Kamer, P. C. J.; Reek, J. N. H.; Dierkes, P. *Chem. Rev.* **2000**, 100, 2741.
- (23) Birkholz, M.-N.; Freixa, Z.; van Leeuwen, P. W. N. M. *Chem. Soc. Rev.* **2009**, 38, 1099.
- (24) Moxham, G. L.; Randell-Sly, H.; Brayshaw, S. K.; Weller, A. S.; Willis, M. C. *Chem.—Eur. J.* **2008**, 14, 8383.
- (25) van Leeuwen, P. W. N. M.; Zuideveld, M. A.; Swennenhuis, B. H. G.; Freixa, Z.; Kamer, P. C. J.; Goubitz, K.; Fraanje, J.; Lutz, M.; Spek, A. L. *J. Am. Chem. Soc.* **2003**, 125, 5523.
- (26) Jeffrey, J. C.; Rauchfuss, T. B. *Inorg. Chem.* **1979**, 18, 2658.
- (27) Slone, C. S.; Weinberger, D. A.; Mirkin, C. A. *Prog. Inorg. Chem.* **1999**, 48, 233.
- (28) Braunstein, P.; Naud, F. *Angew. Chem., Int. Ed.* **2001**, 40, 680.
- (29) Williams, G. L.; Parks, C. M.; Smith, C. R.; Adams, H.; Haynes, A.; Meijer, A. J. H. M.; Sunley, G. J.; Gaemers, S. *Organometallics* **2011**, 30, 6166 and referencetherin.
- (30) Rossi, A. R.; Hoffmann, R. *Inorg. Chem.* **1975**, 14, 365.
- (31) Albright, T. A.; Burdett, J. K.; Whangbo, M. H. *Orbital Interactions in Chemistry*; John Wiley & Sons: New York, 1985.
- (32) Haines, L. M. *Inorg. Chem.* **1971**, 10, 1685.
- (33) Rivers, J. H.; Jones, R. A. *Chem. Commun.* **2010**, 46, 4300.
- (34) Choi, J.-C.; Sakakura, T. *Organometallics* **2004**, 23, 3756.
- (35) Sangtrirutnugul, P.; Stradiotto, M.; Tilley, T. D. *Organometallics* **2006**, 25, 1607.
- (36) Bianchini, C.; Meli, A.; Peruzzini, M.; Vizza, F.; Frediani, P.; Ramirez, J. A. *Organometallics* **1990**, 9, 226.
- (37) Crabtree, R. H. *Acc. Chem. Res.* **1990**, 23, 95.
- (38) Crabtree, R. H.; Lavin, M.; Bonneviot, L. *J. Am. Chem. Soc.* **1986**, 108, 4032.
- (39) Ledger, A. E. W.; Moreno, A.; Ellul, C. E.; Mahon, M. F.; Pregosin, P. S.; Whittlesey, M. K.; Williams, J. M. J. *Inorg. Chem.* **2010**, 49, 7244.
- (40) Cooper, A. C.; Clot, E.; Huffman, J. C.; Streib, W. E.; Maseras, F.; Eisenstein, O.; Caulton, K. G. *J. Am. Chem. Soc.* **1999**, 121, 97.
- (41) Budzelaar, P. gNMR, 4.0; Cherwell Scientific, Oxford, 1997.
- (42) Pontiggia, A. J.; Chaplin, A. B.; Weller, A. S. *J. Organomet. Chem.* **2011**, 696, 2870.
- (43) Pawley, R. J.; Moxham, G. L.; Dallanegra, R.; Chaplin, A. B.; Brayshaw, S. K.; Weller, A. S.; Willis, M. C. *Organometallics* **2010**, 29, 1717.
- (44) Julian, L. D.; Hartwig, J. F. *J. Am. Chem. Soc.* **2010**, 132, 13813.
- (45) Zuideveld, M. A.; Swennenhuis, B. H. G.; Boele, M. D. K.; Guari, Y.; van Strijdonck, G. P. F.; Reek, J. N. H.; Kamer, P. C. J.; Goubitz, K.; Fraanje, J.; Lutz, M.; Spek, A. L.; van Leeuwen, P. W. N. M. *J. Chem. Soc., Dalton Trans.* **2002**, 2308.
- (46) Nieczypor, P.; van Leeuwen, P. W. N. M.; Mol, J. C.; Lutz, M.; Spek, A. L. *J. Organomet. Chem.* **2001**, 625, 58.
- (47) Sandee, A. J.; van der Veen, L. A.; Reek, J. N. H.; Kamer, P. C. J.; Lutz, M.; Spek, A. L.; van Leeuwen, P. W. N. M. *Angew. Chem., Int. Ed.* **1999**, 38, 3231.
- (48) For a graphical representation of the variation in structural metrics for xanthphos complexes see Figures 7 and 8 in ref 29.
- (49) Zuidema, E.; Escorihuela, L.; Eichelsheim, T.; Carbó, J. J.; Bo, C.; Kamer, P. C. J.; van Leeuwen, P. W. N. M. *Chem.—Eur. J.* **2008**, 14, 1843.
- (50) Pangborn, A. B.; Giardello, M. A.; Grubbs, R. H.; Rosen, R. K.; Timmers, F. J. *Organometallics* **1996**, 15, 1518.
- (51) Lubben, A. T.; McIndoe, J. S.; Weller, A. S. *Organometallics* **2008**, 27, 3303.
- (52) Cosier, J.; Glazer, A. M. *J. Appl. Crystallogr.* **1986**, 19, 105.
- (53) Otwinowski, Z.; Minor, W. *Methods in Enzymology*, Vol. 276. *Macromolecular Crystallography, Part A*; Carter Jr., C. W., Sweet, R. M., Eds.; Academic Press: New York, 1997; pp. 307–326.
- (54) Burla, M. C.; Caliendo, R.; Camalli, M.; Carrozzini, B.; Cascarano, G. L.; De Caro, L.; Giacovazzo, C.; Polidori, G.; Spagna, R. *J. Appl. Crystallogr.* **2005**, 38, 381.
- (55) Sheldrick, G. M. *Acta Crystallogr., Sect. A* **2008**, 64, 112.
- (56) Spek, A. L. *J. Appl. Crystallogr.* **2003**, 36, 7.
- (57) Farrugia, L. *J. Appl. Crystallogr.* **1997**, 30, 565.